First Simulations of Pellet Injections into Heliotron J using HPI2

N. Panadero[1], G. Motojima[2,3], K. Nagasaki[4], KJ. McCarthy[1], F. Koechl[5] and Heliotron J team

[1]*Laboratorio Nacional de Fusión, CIEMAT, Madrid, Spain*
[2]*National Institute for Fusion Science, Toki, Gifu, Japan*
[3]*SOKENDAI (The Graduate University for Advanced Studies), Toki, Gifu , Japan*
[4]*Institute of Advanced Energy, Kyoto University, Gokasho, Uji, Kyoto 611-0011, Japan*
[5]*Culham Centre for Fusion Energy, Abingdon, United* Kingdom

Introduction

Plasma core fuelling is a key issue for the development of steady-state scenarios in magnetically confined plasma devices, particularly important for the helical types [1]. The primary candidate is cryogenic pellet injection (PI), which has been used for several decades [2]. However, a detailed understanding of some processes that occur during and after pellet ablation remains outstanding, in particular for non-axisymmetric devices. For them, the complexity of their magnetic fields, compared to tokamaks, make observations and analysis more intricate. With the aim of improving this situation, the stellarator version of the HPI2 code [3–5], redeveloped for W7-X and initially benchmarked on TJ-II [6], has been implemented for the Heliotron J geometry. In this version, the fully 3D magnetic configuration is taken into account when calculating plasmoid drifts by averaging the magnetic gradient along the plasmoid parallel length [6]. HPI2 results are compared here with experimental result from Heliotron J.

Heliotron J

Heliotron J is a flexible medium-sized helical-axis heliotron device with low magnetic shear [7], a major radius, R, of 1.2 m. and an average minor radius, a_0, between 0.1 m and 0.2 m (these correspond to a plasma volume, V_p, of 0.7 m^3). Its maximum magnetic field on the axis, $B(0)$, is 1.5 T, while its rotational transform varies from 0.3 to 0.8. These are achieved by a coil system that consist of a $L = 1$, $M = 4$ continuous helical coil (L is the pole number of the helical coil, whereas M is the pitch number of the field along the toroidal direction), two sets of toroidal coils and three pairs of vertical coils [8]. Discharges, typically ≤ 200 ms, are heated using an Electron Cyclotron Resonance Heating (ECRH) system, which operates at 70 GHz, the second harmonic of the electron cyclotron resonance frequency for $B = 1.25$ T, and provides up to 0.4 MW of injected power [9]. Additional heating systems are available, but not used in this study.

The Heliotron J PI possesses a Gifford–McMahon cycle compact cryocooler (SRDK-415), for *in-situ* pellet formation, and a pneumatic accelerator, for pellet acceleration. Cylindrical pellets, with typical lengths between 1.1 and 1.2 mm, are injected at low speeds, typically 260 m/s,

from the outer side of the device, along straight delivery lines [10]. The injector is equipped with a light gate system, consisting of one laser/photodiode combination per light gate, to determine the pellet speed. In addition, a shadowgraph system, consisting of a CCD camera and a flash lamp with a 180 ns pulse width, is used to confirm the intactness of a pellet [11]. Moreover, dedicated diagnostics are available for pellet injections. For instance, the Balmer H_α ($\lambda = 656.28$ nm) emitted by the neutral, or partially ionized, cloud that surrounds the pellet is followed using a photodiode equipped with a H_α interference filter and, additionally, using a H_α-array diagnostic, with 32 chords and 1 cm spatial resolution at the magnetic axis, thereby permitting localized detection of the pellet emission [11, 12].

Results from HPI2 simulations for Heliotron J

Several hydrogen PI experiments have been performed in Heliotron J, in which pellets of different sizes were injected into different plasma scenarios [11]. In this work, pellet injections into ECRH plasmas are considered for comparison with HPI2 calculations (the nominal pellet trajectory can be found in Figure 1). For that, density and temperature profiles measured with a Thomson Scattering (TS) system [13, 14] before the injection are used as input, as well as experimental pellet speeds.
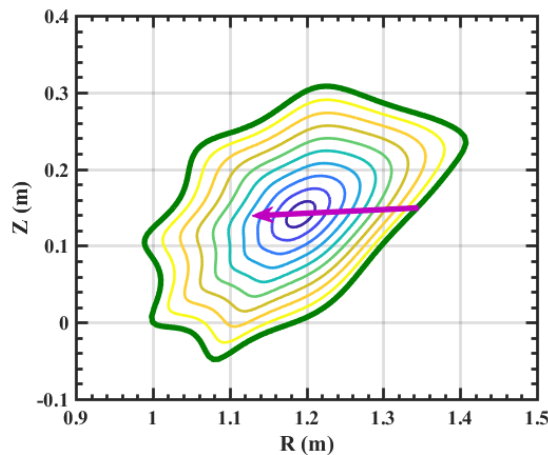
Figure 1. Poloidal cross-section corresponding to the pellet injection port location ($\phi = 22.5^o$). The pellet flight path is shown in magenta (the injection angle is $\alpha = 3.3^o$).

Here, case #79530 is presented. In this case, a 0.7 mm x 0.7 mm cylindrical hydrogen pellet was injected at 290 m/s. In the simulation, a smaller diameter (20% reduction) is considered, to account for a possible erosion along the injection tubes. Electron density and temperature profiles measured by the TS system before pellet injection, and used as input for the simulation, are shown in Figure 2. In addition, an assumed ion temperature profile is shown in this figure.
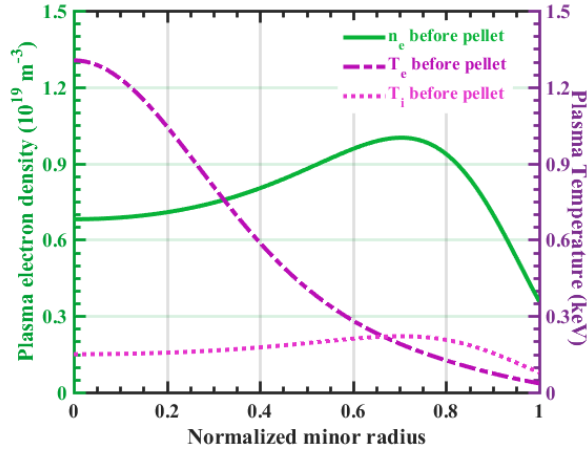
Figure 2. Fitted Thomson Scattering target plasma profiles for #79530 before pellet injection. Left axis) Target density profile in solid green. Right axis) Electron (dash-dot purple) and ion (dot-dot magenta) temperature profiles just before pellet injection.

The obtained ablation profile can be observed in Figure 3, where it is compared to profile reconstructed from the H_α array. The agreement between HPI2 and experimental profiles is reasonably good, considering that the H_α is not directly proportional to the ablation rate. In addition, it should be noted that there may be some uncertainties in the measurement of pellet mass and speed. In addition, the pellet penetration depth, *i.e.*, distance travelled by the pellet until its complete ablation, is well predicted by the HPI2 code.
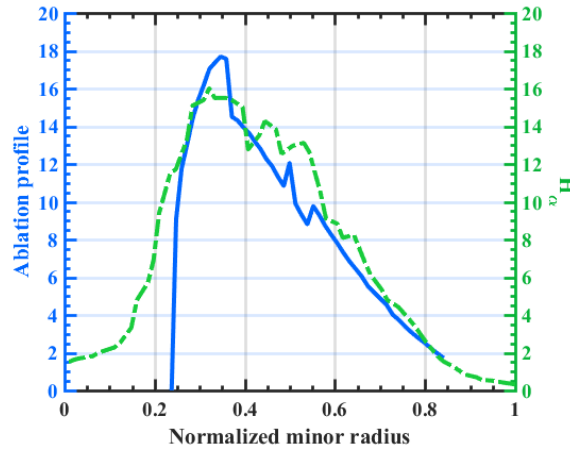

Figure 3. HPI2 simulated ablation (solid blue) profile compared with measured H_α array emission profile (dashed-dotted green) for a pellet of 0.56 mm x 0.7 mm (H content of 9.03×10^{18}) injected at 290 m/s into an ECRH-only plasma (#79530)

Moreover, the post-injection density profile predicted by HPI2 is compared with the density profile measured by the TS 0.5 ms after the pellet injection. They are found in Figure 4, where it is observed that HPI2 density is higher, especially in the outer part, than the TS measurement, although both profiles present similar trends. Moreover, HPI2 density is significantly close to TS measurements, not the fitted profile, for $\rho < 0.6$. In addition, there is a small time difference

between the two profiles, the theoretical and the experimental. Therefore, the time evolution of the predicted density profile, considering transport, may improve the agreement.
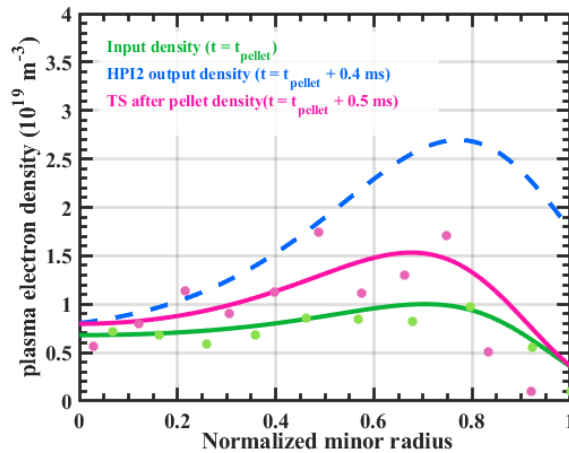

Figure 4. TS electron density profiles measured before (green) and after an injection (magenta) plus density profiles obtained with HPI2 code (dashed blue) for #79530 ($9x10^{18}$ H^0, $v_p = 290$ m/s)

Summary

First simulations of pellet injections for Heliotron J have been performed with HPI2 for a typical ECRH plasma in the standard configuration. The agreement between the predicted ablation profile and the H_α profile is good. In addition, pellet penetration is very well calculated. However, the agreement between calculated and measured density is poorer, although both profiles present similar trends. Moreover, calculating the time-evolution, including transport, of the HPI2 density profile may allow for a better comparison with the TS measurement.

[1]   H. Maaßberg, C.D. Beidler, E.E. Simmet, *Plasma Phys. Control. Fusion* **41** (1999) 1135–1153.
[2]   B. Pégourié, *Plasma Phys. Control. Fusion* **49** (2007) R87.
[3]   B. Pégourié *et al.*, *Plasma Phys. Control. Fusion* **47** (2005) 17–35.
[4]   B. Pegourie, V. Waller, H. Nehme, L. Garzotti, A. Geraud, *Nucl. Fusion* **47** (2007) 44–56.
[5]   F. Köchl *et al.*, *Prepr. EFDA–JET–PR(12)57* (2012) 82.
[6]   N. Panadero *et al.*, *Nucl. Fusion* **58** (2018) 026025.
[7]   T. Obiki *et al.*, *Nucl. Fusion* **44** (2004) 47–55.
[8]   T. Obiki *et al.*, *Nucl. Fusion* **41** (2001) 833–844.
[9]   K. Nagasaki *et al.*, *Contrib. to Plasma Phys.* **50** (2010) 656–660.
[10] G. Motojima *et al.*, *Rev. Sci. Instrum.* **87** (2016) 103503.
[11] G. Motojima *et al.*, *Plasma Phys. Control. Fusion* **61** (2019) 075014.
[12] S. Kobayashi *et al.*, in: Rev. Sci. Instrum., 2006.
[13] T. Minami *et al.*, *Rev. Sci. Instrum.* **81** (2010) 10D532-1–4.
[14] N. Kenmochi, T. Minami, C. Takahashi, *Rev. Sci. Instrum* **85** (2014) 11–819.